

# Resonant Microwave Absorption in an Overdense Plasma Column

G. Böhm

Institut für Experimentalphysik II, Ruhr-Universität Bochum

Z. Naturforsch. **35a**, 293–301(1980); received November 15, 1979

A resonant coupling mechanism is presented which leads to nearly full absorption of an electromagnetic wave in an overdense plasma column. In the resonance case a strong enhancement of the electric field strength within the plasma is found. Under certain conditions this high electric field strength causes parametric excitation of plasma waves in the underdense edges of the discharge. It turned out that the occurrence of this decay process is mainly determined by the density gradients in the plasma.

## I. Introduction

The absorption of microwave power in plasmas is investigated mainly for two reasons: to study heating mechanisms and to produce plasmas without using electrodes. Moreover, since microwave techniques are well developed and easily handled these experiments are performed in analogy to laser experiments.

Of special interest is the problem of the interaction of microwaves with overdense plasmas, i.e. plasmas in which the plasma frequency exceeds the wave frequency. Because of the high reflectivity it was formerly thought to be impossible to produce overdense plasmas with microwave power without superposing a steady magnetic field. But it has been shown experimentally by Beerwald and Kampmann that it is possible to exceed the cutoff density even by more than a factor of 50 ( $\omega_p^2/\omega^2 > 50$ ) in simple microwave devices [1].

In the present paper a method is described profiting from the high reflectivity of overdense plasmas to achieve nearly full absorption. This resonant method leads to a strong enhancement of the electric field strength within the plasma. Using higher microwave power, plasma waves are excited parametrically in the underdense edges of the discharge ( $\omega_p < \omega$ ). Because these regions are characterized by relatively strong density gradients, their influence on the parametric decay process are studied primarily. These observations are compared with theoretical investigations of Flick and Perkins [2].

## II. Propagation of Electromagnetic Waves in Plasmas without Steady Magnetic Field

In the following a short review is given of the propagation of electromagnetic waves in plasmas in the absence of a static magnetic field. From now, electromagnetic waves are always understood to be microwaves. For these frequencies ( $> 10^9$  Hz) the ion motion in the oscillating electric field of the wave can be neglected and only the interaction with the electron gas is taken into account.

Under these assumption the wave propagation in a cold plasma is described by a dielectric constant simply given by

$$\epsilon = 1 - \frac{\omega_p^2}{\omega(\omega - j\nu)}, \quad (1)$$

where  $\omega_p$  is the electron plasma frequency,  $\omega$  the wave frequency and  $\nu$  the frequency for momentum transfer or collision frequency.

The real and imaginary parts of the complex index of refraction  $n = n_r + jn_i$  have the following form [3]:

$$\begin{aligned} n_r &= \left[ \frac{1}{2} \left( 1 - \frac{\omega_p^2}{\omega^2 + \nu^2} \right) + \frac{1}{2} \cdot \left\{ \left( 1 - \frac{\omega_p^2}{\omega^2 + \nu^2} \right)^2 + \left( \frac{\omega_p^2}{\omega^2 + \nu^2} \frac{\nu}{\omega} \right)^2 \right\}^{1/2} \right]^{1/2}, \\ n_i &= \left[ -\frac{1}{2} \left( 1 - \frac{\omega_p^2}{\omega^2 + \nu^2} \right) + \frac{1}{2} \cdot \left\{ \left( 1 - \frac{\omega_p^2}{\omega^2 + \nu^2} \right)^2 + \left( \frac{\omega_p^2}{\omega^2 + \nu^2} \frac{\nu}{\omega} \right)^2 \right\}^{1/2} \right]^{1/2}. \end{aligned} \quad (2)$$

The dependence of  $n_r$  and  $n_i$  on the normalized electron density is shown in Figure 1.

Reprint requests to Dr. G. Böhm, Postfach 102148, D-4630 Bochum-Querenburg.

0340-4811 / 80 / 0300-0293 \$ 01.00/0. — Please order a reprint rather than making your own copy.



Dieses Werk wurde im Jahr 2013 vom Verlag Zeitschrift für Naturforschung in Zusammenarbeit mit der Max-Planck-Gesellschaft zur Förderung der Wissenschaften e.V. digitalisiert und unter folgender Lizenz veröffentlicht: Creative Commons Namensnennung-Keine Bearbeitung 3.0 Deutschland Lizenz.

Zum 01.01.2015 ist eine Anpassung der Lizenzbedingungen (Entfall der Creative Commons Lizenzbedingung „Keine Bearbeitung“) beabsichtigt, um eine Nachnutzung auch im Rahmen zukünftiger wissenschaftlicher Nutzungsformen zu ermöglichen.

This work has been digitalized and published in 2013 by Verlag Zeitschrift für Naturforschung in cooperation with the Max Planck Society for the Advancement of Science under a Creative Commons Attribution-NoDerivs 3.0 Germany License.

On 01.01.2015 it is planned to change the License Conditions (the removal of the Creative Commons License condition “no derivative works”). This is to allow reuse in the area of future scientific usage.

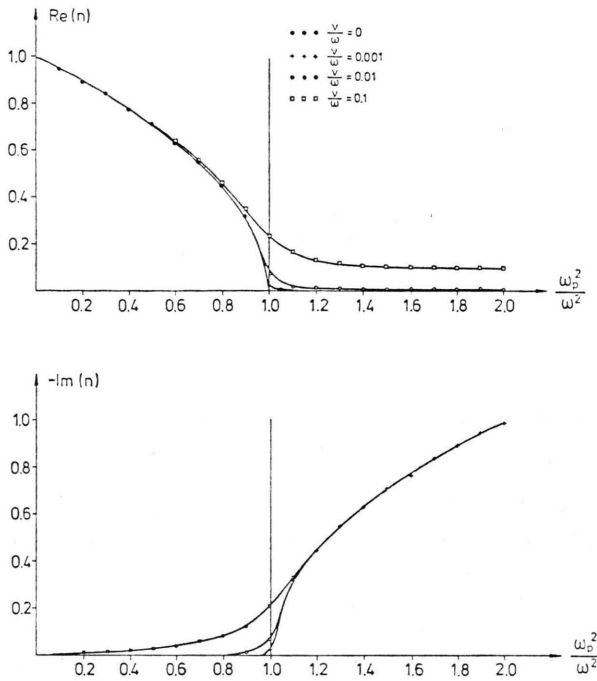


Fig. 1. Real- and imaginary part of the index of refraction versus normalized electron density for various values of the normalized collision frequency.

For non-zero collision frequencies the index of refraction is not purely imaginary for an overdense plasma, but the imaginary part is very large compared to the small real part. Electromagnetic waves propagating in such a medium are therefore evanescent.

### III.1. Incidence of an Electromagnetic Wave on an Inhomogeneous Finite Plasma Slab

Up to now we have discussed the case of wave propagation in an homogeneous infinite plasma. It has been shown that in an overdense plasma the real part of the index of refraction is very small. An incident electromagnetic wave is therefore almost completely reflected at the boundary of the plasma. Only the small fraction of the wave power which really penetrates is strongly damped.

But for a laboratory plasma these considerations are incomplete. Usually we are dealing with plasmas of finite extension exhibiting strong density gradients.

An electromagnetic wave propagates towards a plasma slab which is inhomogeneous in one direction. The inhomogeneity is taken into account by treat-

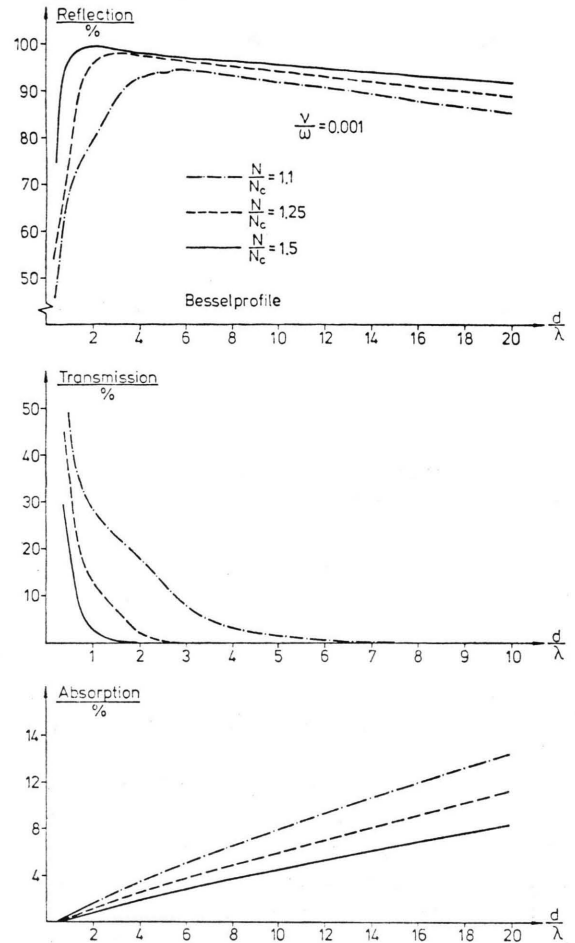


Fig. 2. Reflected, transmitted and absorbed power versus normalized slab thickness.

ing the plasma as a medium being composed of several sheaths with different indices of refraction  $n_k$ . The problem is solved numerically in order to obtain the reflected, absorbed and transmitted power for the whole plasma slab. In all calculations a Bessel profile is considered which is approximated by 30 sheaths. In Fig. 2 the reflected, transmitted and absorbed power is plotted versus the normalized slab thickness.

For a slightly overdense plasma of small extension most of the microwave power is transmitted. With increasing slab thickness and density the transmission is strongly reduced without a significant growth of the absorption coefficient. Now the reflecting properties of the plasma start to play an important role. Good absorption, however, can evidently be achieved by matching with a very flat

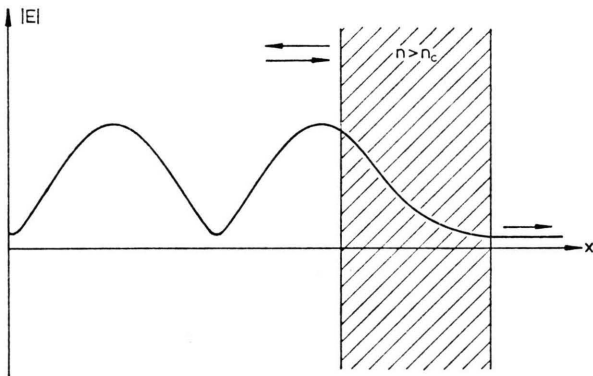


Fig. 3. Schematic distribution of the electric field strength of an electromagnetic wave incident on an overdense plasma slab.

density gradient. But then the microwave power is mainly absorbed in the underdense regions of the plasma. For most purposes high electric field strengths just near the critical density ( $\omega \cong \omega_p$ ) are desired. Figure 3 demonstrates schematically the distribution of the electric field strength of an electromagnetic wave incident on an overdense plasma slab:

The high reflectivity causes a standing wave pattern in front of the plasma slab. The electric field strength penetrates exponentially decreasing into the overdense plasma. Behind the slab an electromagnetic wave with very small amplitude is propagating.

### III.2. Resonant Coupling and Absorption in an Overdense Plasma

Our previous considerations have shown that an effective absorption of electromagnetic waves in a finite partially overdense plasma is impossible because of the high reflectivity. But it is just this feature of the plasma which allows the development of an effective coupling mechanism which leads to almost total absorption. The reflecting plasma slab can be regarded as a slightly permeable mirror (Figure 3). A resonant device can be formed by placing a reflecting wall behind the plasma. The resulting resonator may be compared to a Fabry-Pérot, wellknown in optics. The resonance can be adjusted by choosing the suitable distance between plasma and reflector and by varying the frequency or the electron density. The enhancement of the electric field strength in the plasma then leads to a

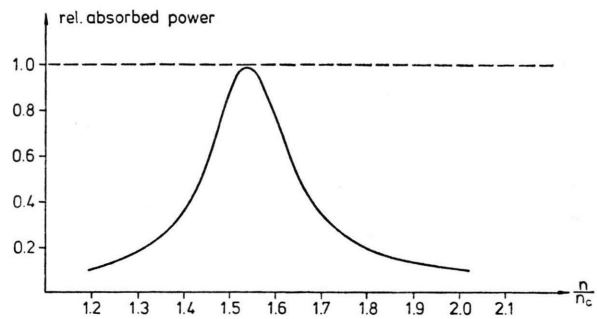


Fig. 4. Calculation of the absorbed power versus normalized electron density in the vicinity of a resonance.

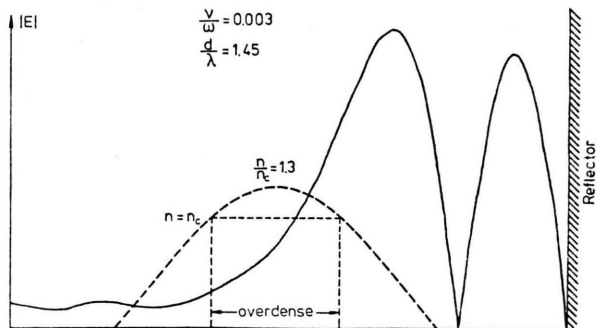


Fig. 5. Calculation of the electric field strength distribution in the resonance case.

strong absorption. In Fig. 4 the absorbed power is plotted versus the electron density in the vicinity of a resonance.

It has already been pointed out that the electric field strength in the plasma is strongly enhanced. The calculated field distribution in the resonance case is shown in Fig. 5 for specific parameters.

Because of the vanishing reflectivity of the resonant system the development of the standing wave pattern in front of the plasma is almost completely suppressed. Within the overdense part of the plasma the electric field strength strongly increases in contrast to the case of no reflecting wall. The field strength maximum is more than one order of magnitude higher than the field of the incident wave. It is located near the critical sheath where the plasma frequency equals the wave frequency. This is an important fact as will be seen later.

### IV. Experiment

In the previous section a method for resonant microwave power absorption in an overdense plasma is described. Experimentally it is easily realized by

means of waveguide techniques. The overdense plasma slab is given by the positive column of a gas discharge located in a rectangular waveguide with the electric lines of force of the excited  $H_{10}$ -mode parallel to the axis of the discharge tube. The waveguide is widened in the field direction mainly to avoid strong radiation losses through the inevitable holes. The reflecting wall is formed by a moveable short behind the plasma column.

We should now give some justifications for replacing the plasma slab and the plane wave in our calculations by the cylindrical plasma column and the  $H_{10}$ -waveguide mode in the experiment. First, the distribution of the electric field strength over the waveguide is given by a sine-function. The discharge tube is placed in the middle of the waveguide and therefore in the most homogeneous part of the field distribution. Second, we compared the results of our calculations with those of Ikegami [4] who exactly solved the problem of a cylindrical plasma column in a rectangular waveguide for the case of pure transmission, i.e. the case with no reflecting wall behind the plasma. In a sufficient wide range of parameters good agreement was found and therefore we avoided these much more complicated calculations.

The schematic experimental setup is shown in Figure 6.

The measurements were made in the frequency range between 4 and 5 GHz. The filling gas was in the pressure range of 1–8 Pa Argon. In the rectangular waveguide the  $H_{10}$ -waveguide mode was excited as mentioned above.

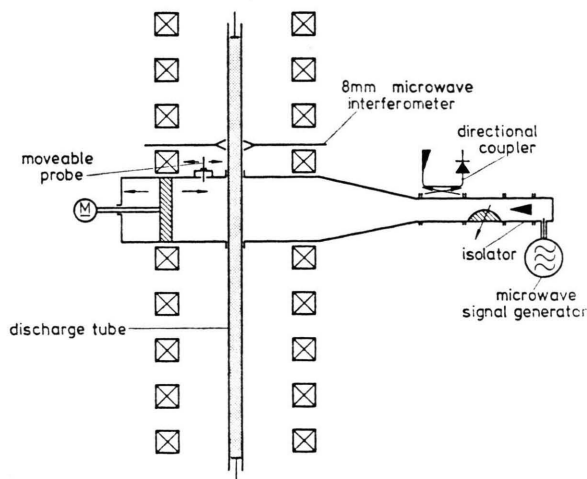


Fig. 6. Experimental setup.

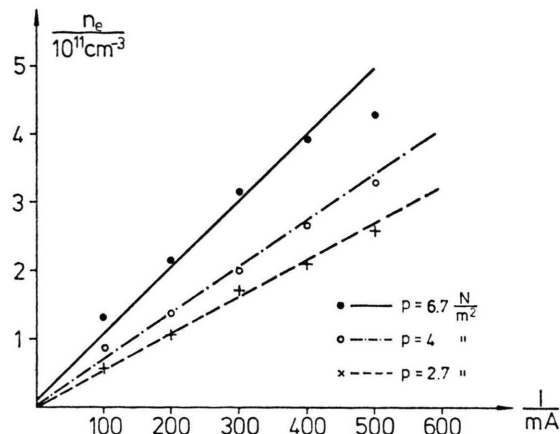


Fig. 7. Electron density versus discharge current for various values of the neutral gas pressure.

It has already been pointed out that the waveguide has been widened in the  $y$ -direction by a factor of seven to keep the losses though the holes small. Therefore the electric field strength is reduced by the same factor compared to the usual dimensions of the waveguide.

The electron density was measured with electrostatic double probes as well as with an 8-mm microwave interferometer. For various filling pressures the electron density versus the discharge current is shown in Figure 7.

The electron temperatures, measured with the double probes, are in the range between 1 and 4 eV.

#### IV.1. Absorption Measurements in the Plasma Resonator

The measurements of the resonant absorption were carried out in the following way: First, the resonance was adjusted roughly by the moveable short; then the frequency was varied symmetrically around the resonance frequency (range:  $\pm 75$  MHz). Using directional couplers the reflected power was determined as a function of the frequency with a microwave network analyzer (HP 8410 A). For various electron densities the results are given in Figure 8.

For increasing electron densities the resonance frequency is shifted towards higher values. This behaviour is easily explained. With increasing density the critical sheath where the plasma frequency equals the microwave frequency is found nearer to the walls of the discharge tube; therefore

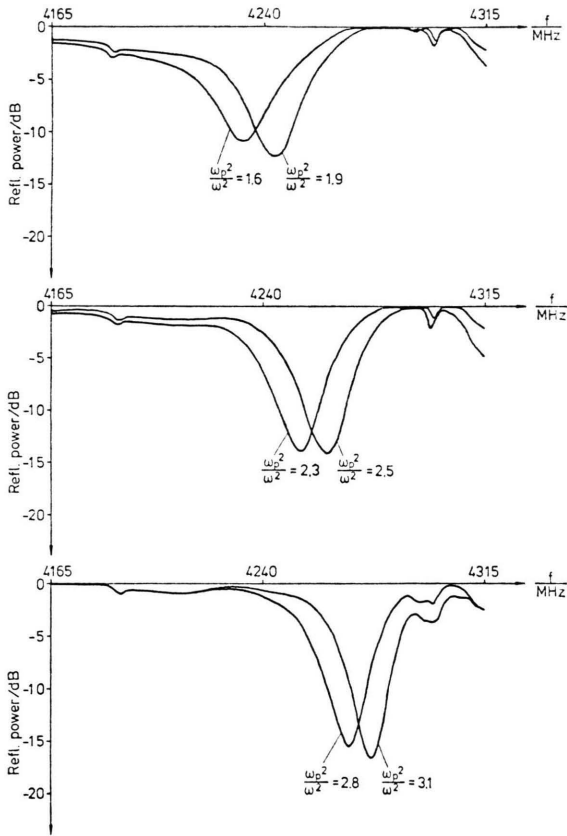


Fig. 8. Reflected power in the vicinity of a resonance for various values of the electron density.

the effective length of the resonator is shortened. Further, higher electron density leads to a weaker coupling and higher  $Q$ -values are expected. Figure 8 demonstrates this effect, too.

If the measured absorption is plotted versus the electron density for constant collision frequency  $\nu/\omega$ , it turns out that in the resonance case easily more than 90% of the incident power is absorbed (Figure 9).

To ensure that neither losses through the holes in the waveguide nor losses in the metal walls of the resonator play an important role, the power coupled through these holes was measured and the  $Q$ -values of a corresponding resonator consisting solely of metal walls was calculated. It was found that the absorption shown in Fig. 9 in fact gives the losses within the plasma column: it should be below total absorption by only a few percent.

From our calculations with the simple plasma-slab-model a considerable enhancement of the

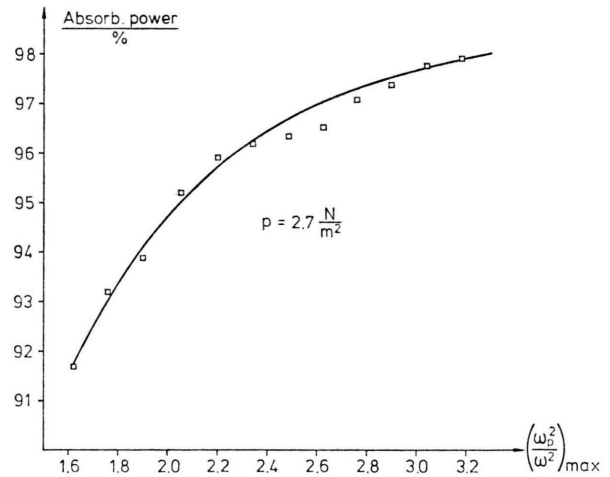


Fig. 9. Resonantly absorbed power versus normalized electron density.

electric field strength is expected. To measure this effect, the waveguide behind the plasma was slotted and a small moveable capacitive probe was inserted. By means of this probe the electric field strength distribution within the resonator could be determined. The result is shown in Figure 10.

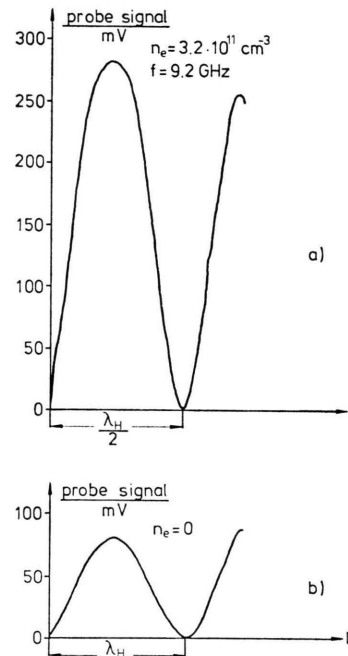


Fig. 10. Measured electric field strength distribution within the resonator a) in case of a resonance, b) without plasma.



The electric field strength in the waveguide for pure transmission is only half of the field strength given in Figure 10b. An enhancement by approximately a factor 7 can therefore be deduced from Figure 10a.

Another method to obtain the value of the electric field strength is the deduction from the measured  $Q$ -values. This is more accurate than the direct measurement and leads to an enhancement of about a factor 10–11 in better agreement with the calculations.

## V. Parametric Excitation of Plasma Waves

The parametric excitation of plasma waves by a sufficiently strong electromagnetic field in a plasma has been investigated by several authors [5–8]. This phenomenon is called parametric decay and nonlinear wave-wave interaction. In the simplest case the interacting waves are the normal modes of the plasma. In a magnetic field-free plasma only three modes exist:

1) The electromagnetic wave, which is described by the dispersion relation

$$\omega^2 = \omega_p^2 + k^2 c^2 \quad (3)$$

with  $\omega_p$  being the electron plasma frequency and  $c$  the velocity of light.

2) The electrostatic plasma wave or Langmuir wave obeying the dispersion relation

$$\omega^2 = \omega_p^2 + 3k^2 v_{th}^2, \quad (4)$$

where  $v_{th}$  is the electron thermal velocity.

3) The low frequency ion-acoustic wave

$$\omega^2 = k^2 \frac{c_s^2}{1 + k^2 \lambda_D^2}, \quad (5)$$

where  $c_s = \sqrt{k_B T_e / M}$  and  $\lambda_D$  is the Debye-length. For long wavelengths the dispersion relation in (5) is simply given by  $\omega^2 = k^2 c_s^2$ .

It can easily be seen from (3) and (4) that the electromagnetic and electrostatic mode can only propagate in an underdense plasma ( $\omega_p < \omega$ ). The parametric excitation of plasma waves is therefore confined to the low density regions of a plasma. In overdense plasma columns usually produced in laboratories strong density gradients are present in these outer regions of the plasma. A good theoretical basis for these experiments should therefore include those density inhomogeneities.

### V.1. Parametric Wave Excitation in Inhomogeneous Plasma

In a qualitative way the influence of a density gradient is easily described. It is well known that for the parametric decay frequency and wave-number matching conditions must be fulfilled,

$$\omega_0 = \omega_1 + \omega_2, \quad k_0 = k_1 + k_2,$$

where the index 0 refers to the so-called pumping wave and the indices 1 and 2 to the parametrically excited plasma waves. In an inhomogeneous plasma the phase-matching condition can only be satisfied in a small region determined by the steepness of the density gradient. The plasma waves leave this region of excitation leading to an energy loss which enhances the threshold field strength.

The parametric excitation of an electrostatic plasma wave and an ion-acoustic wave has been theoretically investigated by Flick and Perkins [2].

Except for the linear density gradient the authors assumed for simplicity, the geometry the calculations are based on, is the same as in our experiment. Flick and Perkins conclude that the decay instability becomes convective in the presence of density gradients. The plasma waves, excited locally, leave the region of excitation before their amplitudes have reached large values. The threshold for an inhomogeneous plasma is given by

$$\frac{\varepsilon_0 E_0^2}{n_e k T_e} \cong \frac{1.6 A (1 + 3 T_i / T_e)}{k_y \cdot L} \left( \frac{\gamma_i}{\gamma_e} \right)^{1/2} + 3.2 \frac{\gamma_i \gamma_e}{\omega_i \omega_e}. \quad (6)$$

The index 0 again refers to the pump field, while the indices i and e are related to the ion-acoustic and electrostatic Langmuir wave respectively.  $L$  is the distance from the plasma edge to the sheath where the electron density reaches the critical density.  $k_y$  is the wave number for both the ion-acoustic and Langmuir wave, because  $k_0 \cong 0$  was assumed. Both plasma waves propagate perpendicular to the density gradient.

In discussing convective instabilities, as threshold value usually the electric field strength is taken leading to growth of the wave amplitudes by a factor  $e^4$ , where  $A$  is taken to be about 5. It can easily be seen from (6) that the threshold value for very flat density gradients, that is for large  $L$ 's, approximates the value for a homogeneous plasma.

A certain confirmation for formula (6) was given experimentally by Eubank in 1973 [9].

## V.2. Experimental Results

In our experiments the positive column of a glow discharge was used as target plasma. The microwave source was a reflex klystron-amplifier in the frequency range between 4 and 5 GHz with a maximum power output of 1.2 kW. The high frequency and low frequency spectra were picked up by two different methods. First, the high frequency spectrum was detected by a suitable waveguide antenna located above the resonator and the low frequency spectrum by means of a capacitive ring placed outside the resonator, too.

Secondly, two coaxial antennas were immersed directly into the plasma column. Both methods yield the same results.

### V.2.1. Frequency Spectra and Threshold

All theoretical investigations mentioned above were performed with the assumption  $k_0 \cong 0$ . In our experiment this condition is fulfilled as well. The parametrically excited plasma waves propagate in opposite directions with  $k_i \cong k_e$ . These conditions together with the dispersion relations lead to a further condition for the frequencies of the excited waves. Simple calculations show that a maximum frequency for the ion-acoustic waves exists which depends on the pump wave frequency and the atomic weight of the gas. This frequency limit can be exceeded only under certain conditions.

In the experiment under consideration ( $f_0 = 4.8$  GHz, Argon) the highest possible frequency of the ion-acoustic wave is 6.4 MHz.

Figures 11a and b show typical decay spectra. Figure 11a shows the high frequency spectrum and Fig. 11b the corresponding low frequency spectrum. Obviously the frequency limit mentioned above is not exceeded.

Calculating the threshold electric field strength for the plasma parameters in the experiment, we obtain 750 V/cm. This is more than one magnitude higher than expected for a corresponding homogeneous plasma. The threshold therefore is mainly determined by the plasma inhomogeneities.

For an experimental proof the apparatus was adjusted to resonance while the incident power was

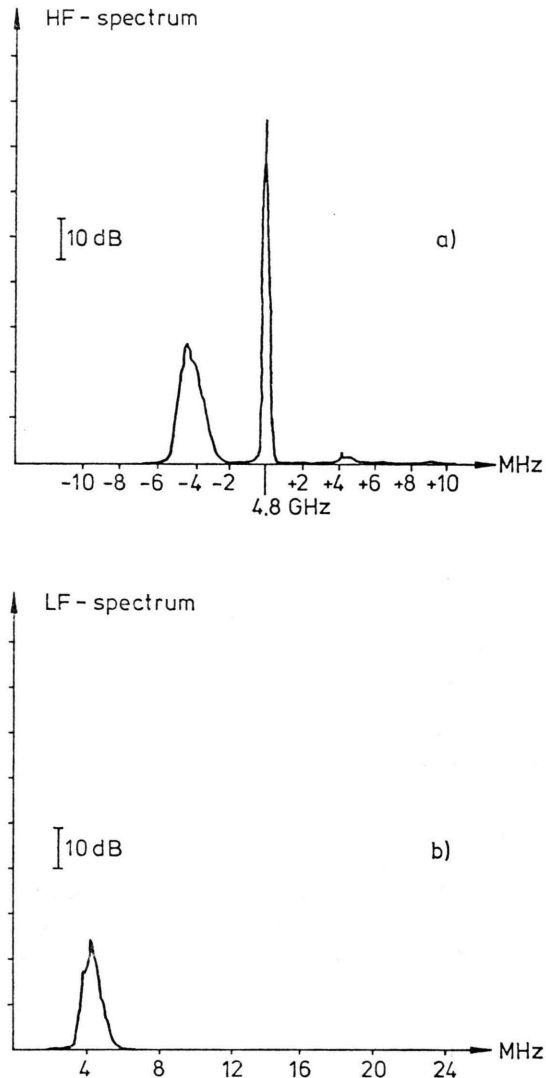


Fig. 11. Decay spectrum a) high frequency spectrum, b) low frequency spectrum.

increased more and more. A threshold-like appearance of the sideband frequencies was observed at about 550 W (Fig. 12) which corresponds to a resonant electric field strength of 680 V/cm.

This measured value is in good agreement with the calculated one, particularly if one keeps in mind the uncertainty in the measurement of the enhancement of the electric field strength and the assumed linear density gradient in the theoretical model.

It has turned out that the threshold for the instability is nearly completely determined by the density inhomogeneities. Therefore no parametric excitation of plasma waves should occur for small

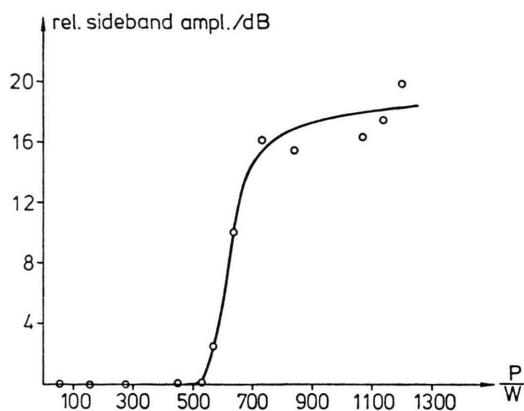


Fig. 12. Relative sideband amplitude versus microwave power.

$L$ 's, i.e. for very steep density gradients. Experimentally this behaviour was investigated. A variation of the  $L$ -value can easily be achieved by simply changing the discharge current. This is shown in Figure 13.

The sideband frequencies do not occur beneath a discharge current of about 450 mA, because the plasma density must first exceed the critical density. From Fig. 8 it can be seen that the electron density at 450 mA is about  $3 \cdot 10^{11} \text{ cm}^{-3}$  at a pressure of  $p \cong 2.7 \text{ Pa}$ . The cutoff density for the microwave in our experiment is  $2.7 \cdot 10^{11} \text{ cm}^{-3}$ . The plasma density is therefore sufficiently high. For discharge currents greater than 1000 mA the density gra-

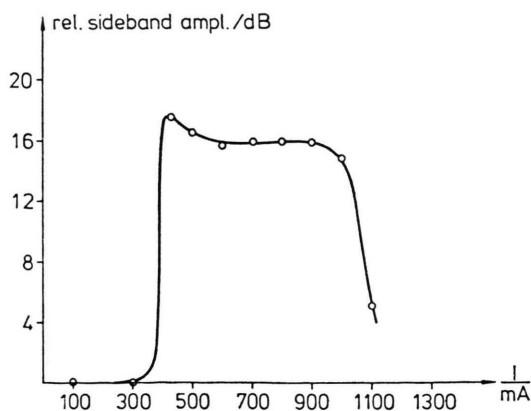


Fig. 13. Relative sideband amplitude in dependence of the discharge current.

dients become too steep and the threshold value can be exceeded no longer. Now an immediate decrease of the sideband amplitudes is observed. This behaviour has been detected qualitatively in several different discharge devices.

## VI. Summary

It has been shown that nearly full absorption of microwave power can be achieved in an overdense highly reflective plasma column if a simple resonance device is used similar to a Fabry-Pérot resonator. If the resonance is adjusted a strong enhancement of the electric field strength within the plasma occurs with its maximum just near the critical density where the wave frequency equals the local electron plasma frequency. This resonance and the connected enhancement of the electric field strength have been shown as well experimentally as in numerical calculations. In a pulsed experiment using very high microwave power ( $p \leq 100 \text{ kW}$ ) the electric field strength within the plasma has been measured spectroscopically by means of the dynamic Doppler effect, leading to the predicted enhancement, too. The results of these spectroscopic measurements will be published elsewhere.

The high electric field strengths just near the critical density favour the parametric excitation of plasma waves if a certain threshold value is exceeded. As theoretically predicted the threshold value for this instability is mainly determined by the density inhomogeneity. In the experiment described here it was higher nearly by one order of magnitude than would be expected for a homogeneous plasma. If the density gradients become too steep, the threshold value will not be exceeded and no plasma waves will be observed.

## Acknowledgements

The investigations have been supported by the Sonderforschungsbereich 162 Plasmaphysik Bochum/Jülich and partially by the DFG Schwerpunktprogramm "Fusionsorientierte Plasmaphysik". The author wishes to thank Prof. Schlüter and Dr. Beerwald for helpful discussions, Dr. Kampmann for his support of the numerical calculations and K. Brinkhoff for his assistance during the experimental work.



- [1] B. Kampmann, Verhandl. DPG (VI) **10**, 285 (1975).
- [2] F. W. Flick, J. Perkins, Phys. of Fluids **14**, 2012 (1971).
- [3] M. A. Heald and C. B. Wharton, "Plasma Diagnostics with Microwaves", J. Wiley, New York 1965.
- [4] H. Ikegami, Jap. J. Appl. Physics **7**, 634 (1968).
- [5] D. Dubois and M. Goldman, Phys. Rev. **164**, 207 (1967).
- [6] K. Nishikawa, J. Soc. Japan **24**, 1152 (1968).
- [7] E. A. Jackson, Phys. Rev. **153**, 235 (1967).
- [8] C. N. Lashmore-Davies, Plasma Physics **17**, 281 (1975).
- [9] H. P. Eubank, Phys. Fluids **14**, 2551 (1971).